Effects of the quasi-biennial oscillation on low-latitude transport in the stratosphere derived from trajectory calculations

H. J. Punge,[1,2] P. Konopka,[3] M. A. Giorgetta,[1] and R. Müller[3]

[1]   The quasi-biennial oscillation (QBO) of stratospheric zonal winds induces a secondary meridional circulation (SMC) consisting of QBO variations in meridional and vertical winds. In this work, we investigate how these instantaneous meridional circulation anomalies add over time to variations of stratospheric transport. To that end, we compute backward parcel trajectories on the basis of the output of a chemistry-climate model (CCM). At the equator, the trajectories show the strongest vertical parcel displacement over a seasonal timescale when the QBO progresses toward easterly phase in the middle stratosphere. During the solstitial seasons a large number of parcels come from the summer hemisphere, causing in addition a QBO variation in the spread of the total ascent among equatorial parcels. A QBO effect on meridional transport is diagnosed from PV gradients during summer in the easterly phase of the QBO, which suggests a variation of the tropical-subtropical barrier strength. Analyses of the parcel trajectories and CCM trace gas distributions confirm this finding. We suggest that this variation is due to the combined effects of QBO and annual variation in meridional advection and in wave-induced eddy transport.

Citation: Punge, H. J., P. Konopka, M. A. Giorgetta, and R. Müller (2009), Effects of the quasi-biennial oscillation on low-latitude transport in the stratosphere derived from trajectory calculations, *J. Geophys. Res.*, *114*, D03102, doi:10.1029/2008JD010518.

1.   Introduction

[2]   The properties of stratospheric air, such as its temperature and composition, are largely determined by the large-scale circulation of the stratosphere commonly referred to as Brewer-Dobson circulation (BDC). Young air that has recently crossed the tropopause undergoes upwelling in the tropical pipe [*Plumb and Bell*, 1982] moves poleward, and descends to eventually re-enter the troposphere. While this simple conception explains many aspects of the real atmosphere, such as the tape recorder signal in water vapor [*Mote et al.*, 1996] or the approximate distribution of long-lived tracers, the real situation is more complicated in a number of ways.

[3]   Firstly, the strength and direction of the circulation varies with time. It is stronger on the winter hemisphere than on the summer hemisphere because of the larger equator-pole temperature gradient in the troposphere that leads to higher wave activity which drives the BDC [*Haynes et al.*, 1991]. The higher level of the wave forcing on the northern hemisphere causes seasonal variations of the tropical upwelling. Furthermore, especially in the tropics and subtropics, the BDC is modulated by the secondary meridional circulation (SMC) of the quasi-biennial oscillation (QBO) [*Plumb and*

Bell, 1982; *Baldwin et al.*, 2001; *Ribera et al.*, 2004], which is illustrated in Figure 1. The easterly (westerly) shear phase of the QBO coincides with enhanced (reduced) upwelling and hence cold (warm) temperature anomalies at the equator [*Reed*, 1964; *Angell and Korshover*, 1964]. This configuration goes along with horizontal divergence and convergence in the QBO easterly and westerly phases and vertical flow anomalies in the subtropics compensating for the equatorial ones. *Niwano et al.* [2003] showed the effect of the QBO on vertical transport as derived from HALOE satellite observations of water vapor and methane.

[4]   Secondly, especially in midlatitudes, air is also dispersed by large-scale planetary waves that cause meridional transport and thereby act to weaken latitudinal gradients and promote the homogenization of air. This effect is most prominent in the midlatitudes of the winter hemisphere, the so-called surf zone [e.g., *McIntyre and Palmer*, 1984; *Plumb*, 2002].

[5]   Vertical wind shear, as, e.g., between the easterly and westerly jets of the QBO, will give rise to the breaking of upward propagating waves over a range of phase speeds and thereby cause mixing. There have been multiple approaches to study the variability of transport. E.g., strong potential vorticity (PV) gradients indicate transport barriers [*Polvani et al.*, 1995], as in the absence of friction and vertical gradients of the heating rate, PV is a conserved quantity. On the basis of a trajectory model study, *Gray* [2000] argued that the characteristics of the subtropical edge of the surf zone depend on the QBO phase. A recent study by *Garny et al.* [2007] found a QBO signal in Lyaponuv exponents calculated from NCEP/NCAR reanalysis winds and indicates that

---
[1]Atmosphere in the Earth System, Max Planck Institute for Meteorology, Hamburg, Germany.
[2]International Max Planck Research School on Earth System Modelling, Hamburg, Germany.
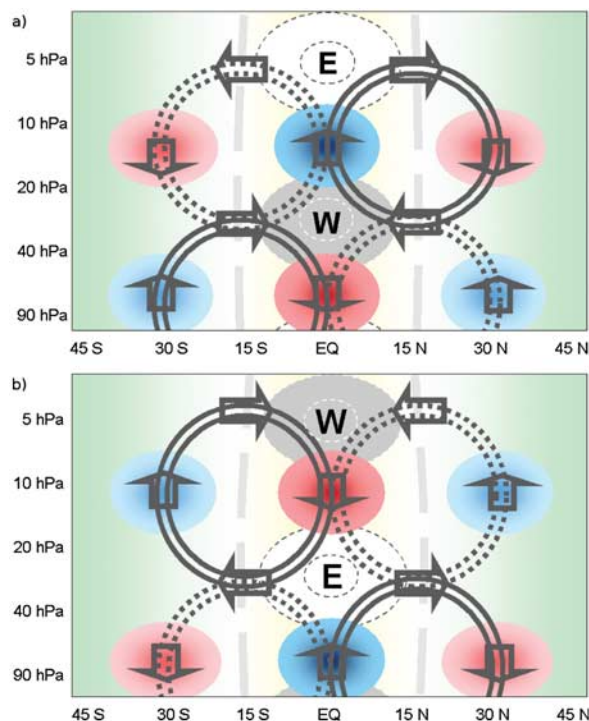[3]Forschungszentrum Jülich (ICG-1: Stratosphäre), Jülich, Germany.

Figure 1. Schematic representation of the secondary meridional circulation of the QBO in analogy to the work of *Plumb and Bell* [1982]. Gray and white fields denote the zonal wind jets, dashed and full arrows the circulation anomaly associated with the QBO corresponding to positive and negative anomalies of the stream function, and red and blue fields the resulting temperature anomalies. (a) Easterly shear phase at 10 hPa; (b) westerly shear phase at 10 hPa. Green (yellow) background shading shows the regions of mean subsidence (upwelling).

mixing at low latitudes is enhanced in summer during the westerly phase compared to the easterly phase.

[6] Mixing caused by such small-scale processes changes the composition of air masses, Several attempts have been made to infer transport properties from trace gas observations. *Neu et al.* [2003] derived the variation of the actual position of the edge from HALOE methane mixing ratios and found that it is mostly due to the annual cycle and the QBO variation is small, in agreement with *Waugh* [1996] and *Chen* [1996]. *Chen* [1996] and *O'Sullivan and Chen* [1996] also found a strong effect of the QBO on planetary wave breaking in winter. Using the concept of "effective diffusivity", *Haynes and Shuckburgh* [2000] and *Shuckburgh et al.* [2001] found propagation of planetary waves to the low latitudes of the summer hemisphere during the westerly phase of the QBO but not during the easterly phase. While these waves are blocked and dissipate at the equator during the easterly phase of the QBO, they propagate across the equator to dissipate at the summer hemisphere easterlies during the westerly phase of the QBO.

[7] Furthermore, concentrations of radiatively active trace gases such as ozone or water vapor, varying either directly because of transport or because of chemical reactions taking place at varying rates [*Tian et al.*, 2006], also affect the circulation via their radiative impact. Similarly, aerosol distributions vary with time and have a radiative feedback.

[8] In this work, we use a modeling framework to illustrate the impacts of the first two listed effects, i.e., the variation of the BDC and the horizontal exchange at the topical-subtropical edge, on transport, with a focus on the role of the QBO. We define the following research questions.

[9] 1. How do the instantaneous QBO-induced variations of the mean meridional circulation translate to anomalies in the long-term transport of air? What are the relative roles of seasonal and QBO variations of the Brewer-Dobson-circulation in the tropics?

[10] 2. How does the QBO affect transport at the tropical-subtropical edge? What is the role of the advection by the horizontal branch of the SMC and the QBO effect on planetary wave propagation?

[11] To study these questions, a novel modeling approach is chosen. Model experiments carried out with the Eulerian chemistry-climate model (CCM) MAECHAM4-CHEM (ME4C) [*Manzini et al.*, 2003; *Steil et al.*, 2003] describe the dynamics of the stratosphere including the QBO, taking into account feedbacks due to chemistry.

[12] This model alone offers limited capabilities to assess transport effects. Therefore the output of the ME4C model is used to drive the Chemical Lagrangian Model of the Stratosphere (CLaMS) [*McKenna et al.*, 2002] to study pathways of air masses for different phase combinations of the quasi-biennial and annual cycles. In this work, only the trajectory module of this model is used. The approach is hence similar to that of *Gray* [2000], but calculations are carried out over a longer time period in order to better separate the effects of QBO and annual cycle and underline their significance. In addition, a reference simulation with no QBO representation is evaluated.

[13] With this setup, it is possible to assess how exactly the equatorial circulation anomalies that are linked instantaneously to the QBO jets, transform to transport anomalies in the tropical region. It is also suited to test the understanding of properties of barriers to horizontal transport suggested by the dynamics and observed trace gas gradients, analyzed e.g., by *Polvani et al.* [1995] and *Shuckburgh et al.* [2001] in a purely Eulerian framework. The Lagrangian view taken with the calculation of trajectories allows for a more process-based understanding of the transport effects and provides a link from diagnosed circulation anomalies to the resulting anomalies in trace gas distributions.

[14] In the following section, the model framework used will be explained in detail. The third section focuses on the impact of the QBO on vertical transport, while the fourth assesses the impact on horizontal transport. Conclusions are discussed in section 5.

2. Modeling Approach

2.1. Chemistry-Climate Model Simulations

[15] For the Eulerian calculations, the chemistry climate model MAECHAM4-CHEM [*Manzini et al.*, 2003; *Steil et al.*, 2003] is used. It consists of the middle atmosphere general circulation model MAECHAM4 [*Manzini et al.*, 1997], which is based on ECHAM4 atmosphere general circulation model. [*Manzini and McFarlane*, 1998; *Roeckner et al.*, 1996]. Effects of orographic gravity waves are parameterized following [*McFarlane*, 1987], and the Doppler spread formulation of [*Hines*, 1997a, 1997b] is used to

parameterize the effects of a broad band spectrum of non-orographic gravity waves. The radiation scheme as described by *Roeckner et al.* [1999] is interactively coupled to concentrations of methane, N_2O and ozone from the chemistry model CHEM [*Steil et al.*, 1998]. Simulations are carried out in the version with spectral truncation T30, associated with a Gaussian grid with a spacing of 3.75° and 39 vertical layers, of which the uppermost is centered at 0.01 hPa.

[16] The two model experiments used in this work, running from 1980–1999, also described in *Punge and Giorgetta* [2008], differ chiefly in the representation of the QBO. While MAECHAM4-CHEM has no QBO in the free-running setup, an accurate and consistent representation of the QBO and its effects can be obtained by the nudging of equatorial stratospheric winds [*Giorgetta and Bengtsson*, 1999] as applied in this work. This allows for a comparison of transport in largely similar model simulations with and without QBO representation.

[17] In both experiments, sea surface temperatures from the HadISST1 data set [*Rayner et al.*, 2003] and greenhouse gas and halogen emissions as in the WMO/UNEP assessment 2002 [*WMO*, 2003] are used as lower boundary conditions.

[18] The first experiment ("non-QBO") is free-running and does not produce an intrinsic QBO at the given vertical resolution. The second experiment ("QBO") is in contrast forced to have a QBO equivalent to observations using the nudging technique: Winds in the tropical stratosphere are relaxed linearly toward the observed wind record from the Singapore radiosondes, which are launched close to the equatorial maximum of the QBO. The applied forcing is zonally uniform with a Gaussian profile around the equator with a full width of half maximum ranging from 20° at 70 hPa to 30° at 10 hPa. Observations from seven altitude levels between 70 and 10 hPa are used until 1986, when measurements on 14 levels between 90 and 10 hPa became available. Above 10 hPa, the vertical propagation of the QBO jets in the forcing is continued at a constant rate, but with decreasing strength. The nudging applied here neglects hemispheric asymmetry of the QBO in zonal wind and produces easterly and westerly jets of equal width. This is a limitation of the model, and as a consequence, e.g., the exact location of horizontal transport regimes may differ slightly from that in reality. Zonal asymmetries are also assumed to be negligible.

[19] In addition, in the nudged experiment, solar activity is parameterized using radiation flux data of *Lean et al.* [1997] and the aerosol forcing caused by volcanic eruptions is included by prescribing pre-calculated net heating rates of *Kirchner et al.* [1999] and the surface area densities of *Jackman et al.* [1996] for the chemistry module. These two observational forcings were not included in the simulation without QBO nudging. The forcings are additional sources of interannual variability in the QBO run, mainly by introducing effects of the 11-year solar cycle and the eruptions of El Chichon in April 1982 and Mt. Pinatubo in June 1991.

[20] In this study, the impact of the 11-year solar cycle [e.g., *Tourpali et al.*, 2003] can be neglected, as most considerations here are on shorter time scales and the effect is small in the considered altitude range anyway. The volcanic eruptions do however impact transport because of the heating effects caused by aerosols [e.g., *Trepte and Hitchman*, 1992; *McCormick et al.*, 1995]. Consequently, a significant slowdown of the BDC is observed in the "QBO" model run after

the eruption, and for this reason, the post-eruption periods are not suitable for the elaboration of QBO effects.

[21] The nudged experiment has previously been evaluated within the SPARC CCMVal activity [*Eyring et al.*, 2006] on the validation of chemistry-climate models, which revealed some deficiencies in the methane and water vapor concentrations in the model. On the other hand, in a slightly different experiment, *Steinbrecht et al.* [2006] found good agreement of modeled and observed temperatures and total ozone values. Similarly, *Punge and Giorgetta* [2008] found a good representation of the QBO effects on temperature and ozone in the simulation used here. Hence despite the rather coarse horizontal resolution of the CCM with about 8 grid points in the QBO region, the secondary meridional circulation seems to be realistic. The results of these studies indicate that stratospheric dynamics and its variability is generally well represented in the model; trace gas distributions may however suffer from deficiencies in the CCM's transport and chemistry schemes.

[22] For using the CCM output within the CLaMS setup, some processing is required. Zonal and meridional wind components, temperatures and net heating rates are extracted and interpolated from the hybrid pressure-height coordinate σ of the ME4C model to the vertical coordinate ζ of the CLaMS model, which is a hybrid of pressure p in the troposphere and potential temperature θ in the stratosphere [*Konopka et al.*, 2007]. At the levels considered here, $\zeta = \theta$ and $\sigma = p$.

2.2. Transport Barriers

[23] In Figure 2 we use potential vorticity (PV), computed on isentropic levels, to illustrate the difference between the two model runs. PV is close to zero at the equator, and increases (decreases) toward the North (South) pole. Its meridional gradient is not uniform though, and, as noted before, strong gradients indicate transport barriers, while weak gradients indicate a well-mixed region. Following *Nash et al.* [1996], the singular points of the second derivative of PV along equivalent latitudes can be used to define a latitudinal barrier.

[24] Figure 2a shows the daily averaged PV gradient at the 600 K ($\approx$32 hPa) over several years in the run including the QBO, Figure 2b in the run neglecting the QBO. In both cases, the increased PV gradient at the winter vortex edge on both hemispheres can clearly be discerned. At lower latitudes, in the non-QBO run, PV gradients are strongest around the equator, with a tendency toward the summer hemisphere, suggesting a transport barrier there. There is a region of notable PV gradient at around 20°N (15°S) during northern (southern) winter that migrates toward 35°N (30°S) during spring and summer to form the edge between the relatively well-mixed regions of subtropical summer easterlies and summer high latitudes.

[25] At mid-latitudes, there is considerable variability in PV, especially during fall, and the winter time surf zone appears to develop thoroughly only by midwinter. The variability of the winter PV field is a consequence of the exchange of air masses from the near tropics and the mid-latitudes. The large-scale eddies generated by the planetary waves, which are strong on the winter hemisphere (especially the northern), cause transport on a time scale of several days and leave an imprint on PV gradients, even though equivalent
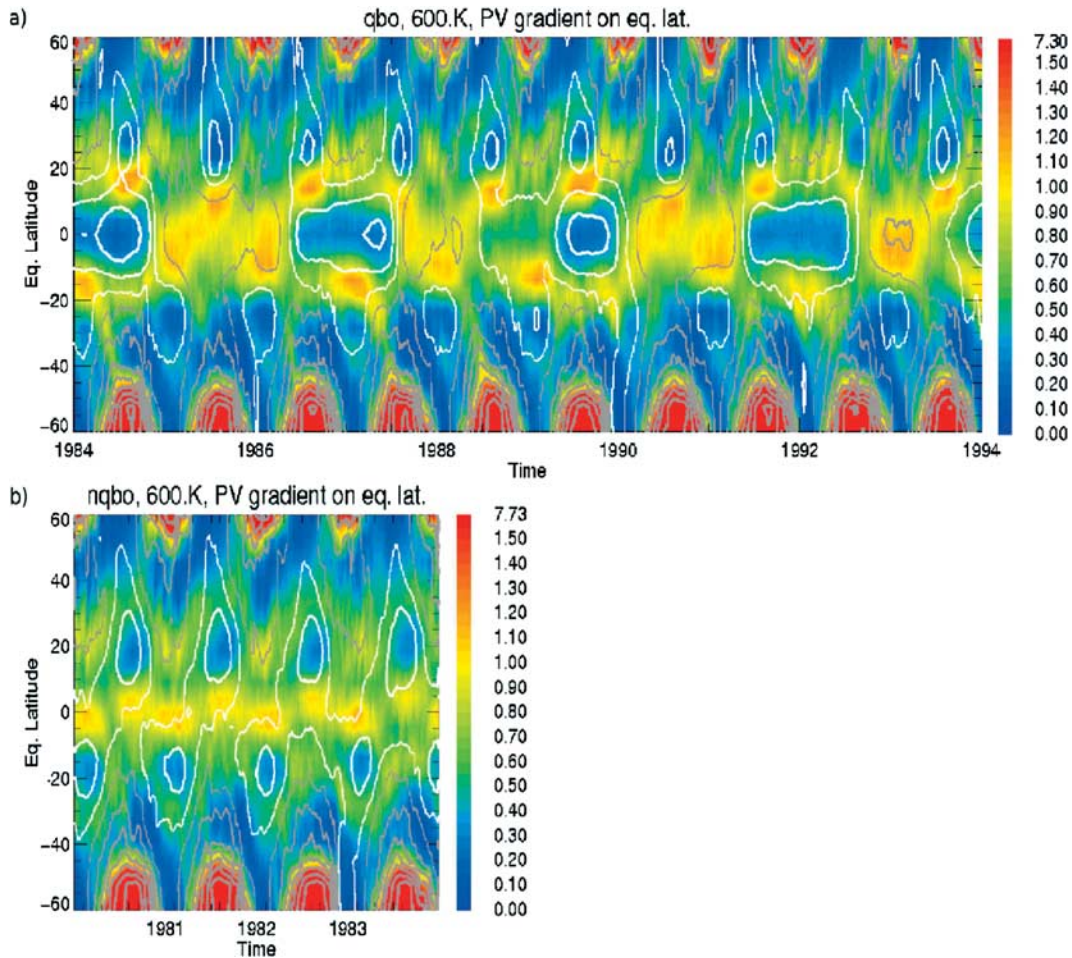
Figure 2. Shades show the horizontal gradient of potential vorticity, as analyzed at the 600K (≈32 hPa) potential temperature level: (a) QBO experiment; (b) non-QBO experiment. Gray contours denote westerly zonal wind at 5, 15, 25, 35, 45, 55, and 65 m/s, while white contours show easterlies with the same spacing.

latitude is used in Figure 2. Corresponding variability is also seen in the (10-day averaged) zonal wind field. The planetary waves from the winter hemisphere appear to reach up to the edge of the subtropical easterlies in the summer hemisphere, where they are damped and a barrier is established [*Haynes and Shuckburgh*, 2000].

[26] Interestingly, the situation in the QBO run is similar to the non-QBO case during the westerly phases, just the subtropical PV gradients are smaller. The westerly winds allow the planetary waves to propagate through the equatorial region, but are damped where winds become more easterly (e.g., slightly north of the equator in 1985) causing a barrier as discussed by *Shuckburgh et al.* [2001].

[27] When there are easterlies though, there is no PV gradient in the tropics between 10°S and 10°N. This can be understood by considering the latitudinal part of the meridional circulation (Figure 1). During the easterlies, equatorial, low PV air is moving poleward. There is a strong PV gradient at the summer edge of the easterly QBO jet, and again a weak PV gradient in the subtropical summer easterlies. The apparent barrier in the summer subtropics, for which there is no clear evidence in the work of *Gray* [2000], can however hardly be generated by planetary waves from the winter hemisphere, as these are blocked by the strong easterly jet.

[28] We find that it is difficult to explain the observed transport variations from the analysis of PV fields alone. The trajectory calculations allow to analyze latitudinal transport in detail and to deduce the integrated effect over a longer time period. This will be done in section 4, with a focus on the barrier diagnosed at the summer edge of the easterly QBO jet.

2.3. Trajectory Calculations

[29] Because of the modular structure of CLaMS, the trajectory module of CLaMS can be used for stand-alone calculations. It uses a fourth-order Runge-Kutta algorithm to infer the motion of air parcels from winds and heating rates [*McKenna et al.*, 2002]. Trajectories are started on a regular $1° \times 1°$ grid between 80°S and 80°N, omitting the polar regions. The total number of trajectories on each level is $360 \times 160 = 57,600$. The time step for the trajectories is 30 minutes.

[30] Four isentropic levels (500, 600, 675, and 870 K, corresponding to about 50, 32, 20, and 9 hPa) were selected to compute backward trajectories over 90 days. At low latitudes the impact of mixing over such a time span is assumed to be small enough for the trajectory distribution to give a reasonable representation of the origin of the air that is found at these levels. Starting dates were chosen at four

dates at the end of January, April, July and October over several years in order to represent the seasonal differences and the interannual variations in both the QBO and non-QBO experiments.

[31] The combined modeling approach chosen here has several advantages compared to using operational analysis or reanalysis to drive the CLaMS model. The isentropic ascent rates can be taken from the model calculation directly rather than being inferred from often noisy analyzed vertical wind.

[32] The full CLaMS model can be used for extensive Lagrangian studies of the stratosphere [e.g., *Konopka et al.*, 2007; *Khosrawi et al.*, 2005], and the modeling approach presented here offers the possibility of further, more detailed analyses based on Eulerian calculations.

3. QBO Effects on Vertical Transport

[33] To analyze how transport within the tropics is affected by the QBO, the backward trajectories of parcels starting at the 870 K level, corresponding to 9 hPa, in the tropics between 12°S and 12°N are considered, hence of $24 \times 360 = 8640$ parcels. In the QBO model run, for a given start date, years with pronounced easterly wind, westerly shear, westerly wind or easterly shear phase of the QBO at that level were selected. A case from the CCM simulation with no QBO is given for comparison. No significant hemispheric asymmetries are expected, also because of the symmetric QBO forcing applied in the model, and hence we will show examples for the boreal spring and summer cases at this point.

[34] We start out presenting the results for trajectories run during an equinoctial season, when the circulation is expected to be approximately symmetric about the equator. Figure 3 shows the distribution of trajectories calculated backward from 28 April. The location of the air parcels in the meridional plane is depicted in 30-day intervals after binning them to a $1 \text{ K} \times 1°$ grid. The resulting density distribution is smoothed by a simple filter and cut off at 0.1 for a smoother display. The rate downward propagation of a parcel cloud when going back in time hence reflects the rate of ascent of air.

[35] The overall ascent of parcels over the course of 90 days can be inferred from their mean altitude at day −90 (solid line in Figure 3). The air is ascending by 150 to 250 K, depending on the QBO phase. Total ascent is weakest for the trajectories started in the westerly shear phase (WS, Figure 3d) but strongest in the easterly phase (E, Figure 3c). From the secondary meridional circulation (SMC, see Figure 1), one would have expected the strongest ascent during easterly shear. However, the circulation pattern of the SMC depicts only the motion at one instant, while for transport of air parcels, their history needs to be considered. Air parcels, while following the general upwelling in the tropical pipe, subsequently enter the downward propagating QBO shear zones and jets, in which the circulation may differ considerably, as will be discussed in more detail below.

[36] The shape of the distribution also differs distinctly among the cases. It is evident from the shear cases in Figures 3b and 3d that the modulation of upwelling by the SMC is strongest at the equator and has an approximately Gaussian profile, as the QBO itself. Over the course of 90 days, these meridional differences apparently level off by horizontal dispersion, and the mean potential temperature is approximately

the same in the entire equatorial region. We also note that the initial dispersion of the parcels upon their release is stronger in the shear phases than in the easterly and westerly wind phases. This suggests that the conditions are more favorable for mixing of air masses in these phases.

[37] Furthermore, as can be inferred from the shape of the 3% percentiles of their horizontal distribution (dashed lines in Figure 3), while the parcels mostly originate from within 15°S to 15°N in the easterly case, they stem from the 25°S to 25°N range in the westerly case and the westerly shear case. This is the effect of the equatorward motion associated with the westerly phase (Figure 1).

[38] The Brewer-Dobson circulation (BDC) is hemispherically asymmetric during the solstitial seasons, which affects also transport at tropical latitudes. Figure 4 shows the same distributions of air parcels as Figure 3 but for release of parcels on 28 July and for different years but with similar QBO phases as above. It is evident from Figure 4 that air masses ascending in the equatorial region during this time of the year are influenced by the seasonal circulation anomaly. Most of the parcels originate from the northern subtropics, which is due to the extension of the southern cell of the BDC to the northern hemisphere during boreal summer. Only for the parcels that come from the tropics, the upwelling is different between easterly and westerly shear cases, as for the equinox case. Also note that the parcel distribution is spread out on the extratropical winter hemisphere especially in the westerly case and the easterly shear case, which is likely because of perturbations caused by planetary waves propagating from higher latitudes. When the tropical wind is easterly, these waves cannot propagate and are blocked from the tropics. Also, slightly more parcels stem from the 10°N−30°N range in the westerly phase, which is again interpreted as the effect of the SMC. However, planetary waves from the winter hemisphere may also cause dispersion of the trajectory groups in this region [*Chen*, 1996; *Shuckburgh et al.*, 2001]. The various effects of the shear phases of the QBO on circulation and transport are summarized in Table 1.

[39] While the selected cases presented in Figures 3 and 4 give a clear impression of the QBO under solstice and equinox conditions, it is also useful to investigate the variability of the ascent because of the combination of seasonal and QBO cycle over a longer time period. To that end, the course of backward trajectories that arrive at three selected levels within ±2° off the equator was analyzed in three month intervals over a period of ten years covering various phase states of the QBO, and for the experiment with no QBO. At each date, $360 \times 4 = 1440$ parcels start in this region. Figure 5a illustrates the ascent of parcel ensembles driven by the QBO simulation and Figure 5b the corresponding ascent in the simulation with no QBO. Trajectories are started at 500, 675, and 870 K on 28 April, July, October and January from 1984 till 1994 in the QBO simulation and in the period 1980–1984 in the non-QBO simulation. The median altitude of the groups of trajectories is given by the solid line and the altitude range between the 10th and 90th percentiles of the vertical distribution of the parcels is colored by season. The curvature and ascent of the lines clearly depend on the QBO phase which can be inferred from the zonal wind shown in the background; gray shading marks westerly wind, while white shades stand for easterlies.
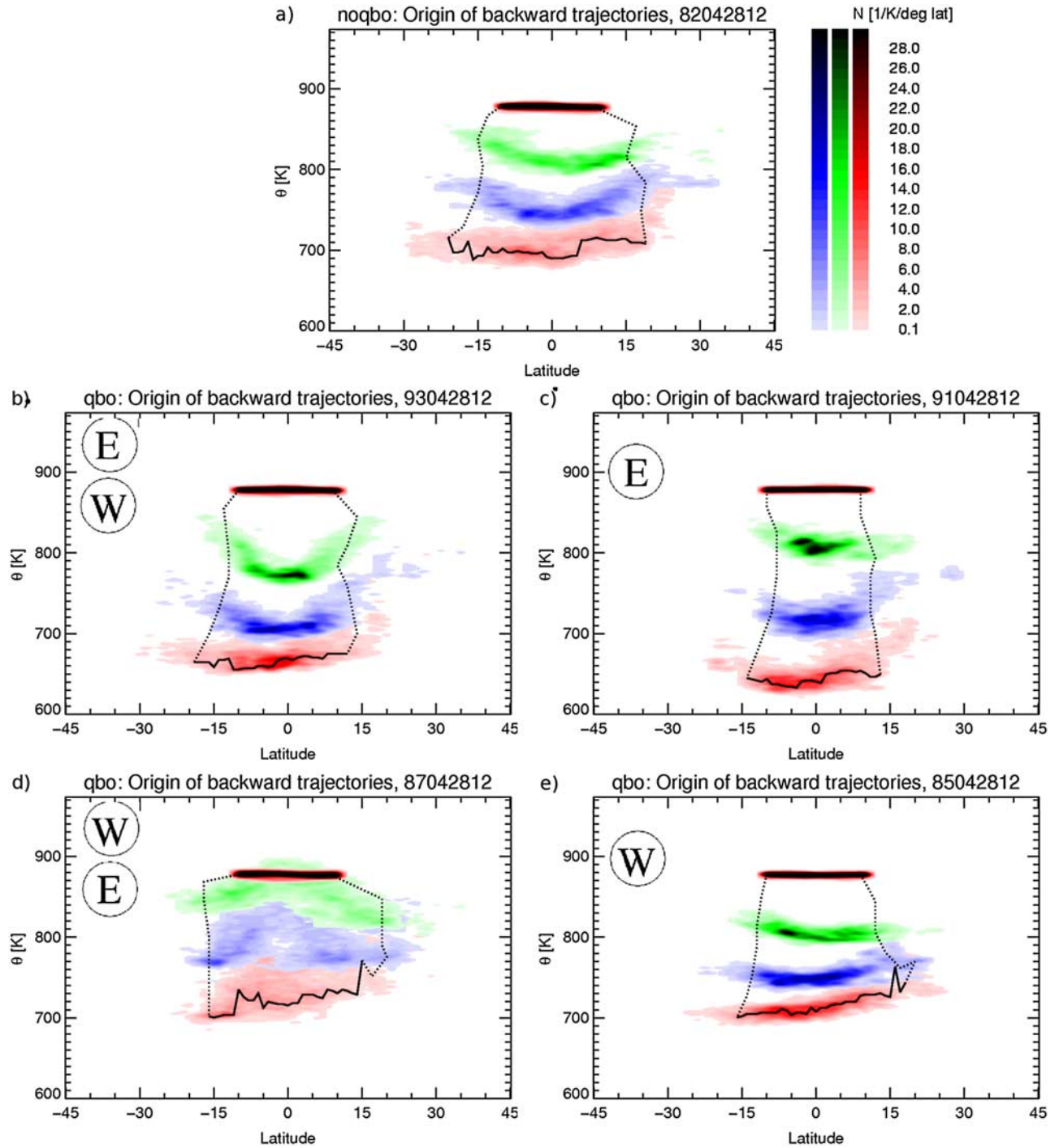
Figure 3. Density distribution of backward trajectories starting at 870 K on 28 April, depicted in 30-day intervals in different colors to illustrate the propagation. (a) Trajectories in spring of 1982 in the model that does not have a QBO representation. For the QBO model 4 years were selected that have a well-defined QBO phase at 870 K: (b) 1993, easterly wind shear; (c) 1991, easterly wind; (d) 1987, westerly wind shear; (e) 1985, westerly wind. The two dashed lines are chosen such that 3% of the parcels are located north and south of them, respectively, at each time step; the solid line gives the mean altitude for parcels at day 90 of the calculations.
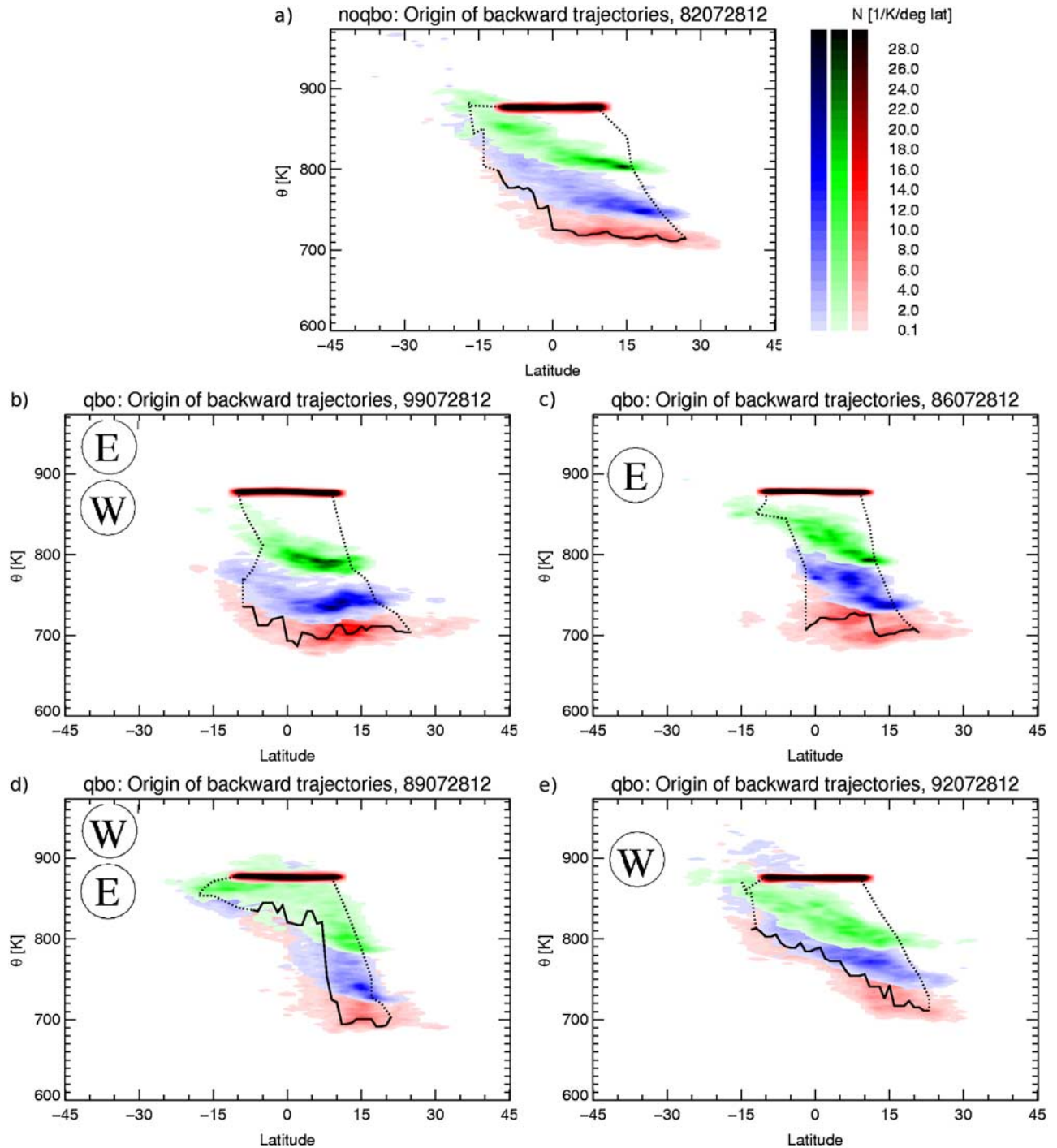
Figure 4. As in Figure 3 but for trajectory runs started 28 July: (a) no QBO (1982); (b) easterly shear (1999); (c) easterly wind (1986); (d) westerly shear (1989); (e) westerly wind (1992).

[40] In the case with no QBO, shown in Figure 5b, the annual cycle in the vertical trajectory distributions is clearly seen. It is due to the annual variations in both upwelling and horizontal transport of air parcels. Ascent differs by about a factor of two between trajectories started in July and those started in April. Especially at higher levels, a considerable fraction of parcels is advected to the equator from the subtropics over 90 days in the solstitial seasons, as seen in Figure 4, which causes the higher width of the parcel distributions in these seasons.

[41] In Figure 5a, the additional variability due to the QBO is seen. Figure 5a shows clearly how parcels ascending in the tropics move through the different descending QBO phases. While the QBO phase difference between 400 and 870 K (70 and 9 hPa) at any instant is about π, the parcel will usually undergo a full QBO cycle within about one year when traveling between these two levels because of the change in the QBO phase during the travel.

[42] Assuming a parcel stays within the tropics, its cross-isentropic vertical motion will be determined by the local

Table 1. Summary of Effects of QBO Shear Phases on Circulation and Transport

	Quantity	Easterly Shear	Westerly Shear
1	Instantaneous equatorial upwelling	Enhanced	Reduced
2	Total tropical ascent over 90 days	Enhanced, delayed w.r.t. 1	Reduced
3	Horizontal spread in ascent among parcels in solstitial seasons	Small	Large
4	Parcel distribution	Compact	Disperse

heating rates, which vary with the QBO, and the ascent of a parcel is the integral of the heating rates experienced. When parcels start in the easterly phase at 870 K, as in April 1991 (also see Figure 3c), they have ascended from an easterly shear phase (ES) before and experienced strong ascent there. At the same time, the parcels started in the ES phase, as in April 1993 (also see Figure 3b), although their ascent was the strongest for the first 30 days of the calculation, have come from a westerly jet, where ascent was slower, which explains why the total ascent over 90 days was higher in the easterly case than in the ES case in Figure 3. For the westerly (W, Figure 3e) and westerly shear (WS, Figure 3d) phases, the ascent rate was lower, and so was the QBO phase difference between the start and the end of the trajectories. Thus the effect of the integration over 90 days is lower, explaining that the WS phase case has the lowest total ascent over the 90-day period.

[43] Due of the change of the circulation with time, cases with no ascent over 90 days are rarely found, despite the occurrence of weakly negative heating rates during the
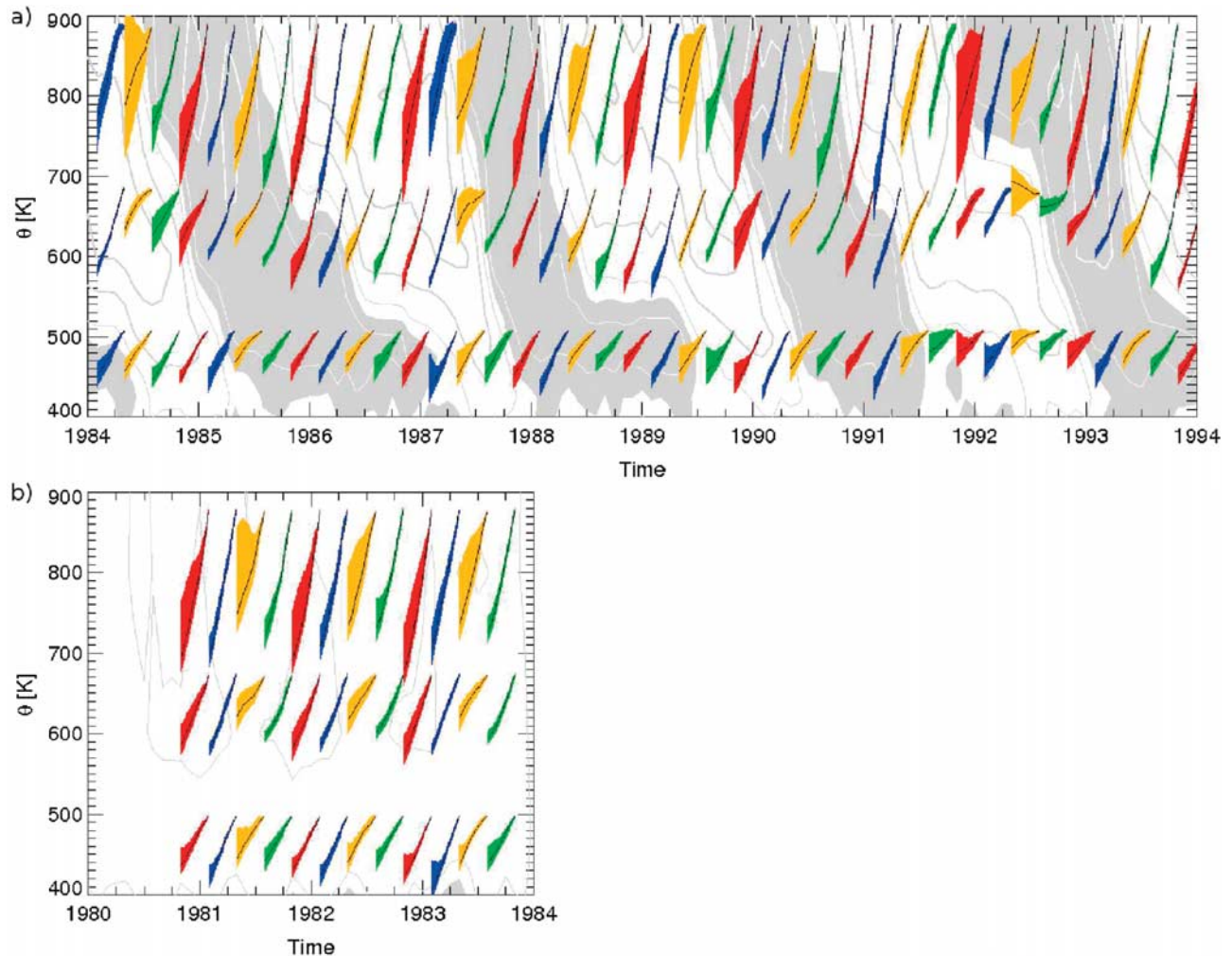

Figure 5. (a) Vertical transport of air parcels within [2°S, 2°N] in the QBO model. Stripes represent the course of the backward trajectories started at various dates from the 500-, 675- and 890-K levels. The solid line marks the median vertical positions of the air parcel groups during 90 days before their arrival at the start level, while the 10th and 90th percentiles of the group bound the colored stripes. The colors stand for the starting date: red for 28 January, blue for 28 April, yellow for 28 July, and green for 28 October. The zonal wind fields in the background show the descending westerly (gray shading with white contours at 5, 15, and 25 m/s) and easterly (white shading with gray contours at 5, 15, 25, and 35 m/s) QBO jets. (b) Same as Figure 5a but for the experiment with no QBO representation.

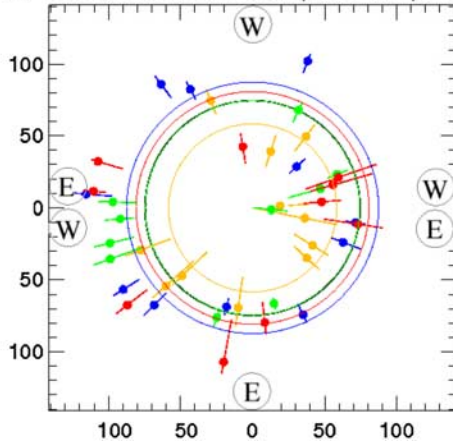qbo, 675.K, 50th/10th/90th perc. vs qbo phase

Figure 6. Polar plot of ascent vs. QBO phase. The radii of the circles give the mean ascent of the 675-K air parcels as in Figure 5a over the course of 90 days in K. The black one stands for the climatological average of all starts over the 7 years and colors distinguish between seasons as in Figure 5. Marks with bars stand for the individual trajectory runs and are plotted at the QBO phase at the start of the trajectory calculations. They give the median and 10th/90th percentiles of the vertical distribution at day 90. The QBO phase is rotating counterclockwise and is westerly on the positive ordinate.

westerly shear phase. One exception is found in the parcels released at 675 K in July 1992, which may however be affected by the anomalous heating rates caused by the anomalous aerosol load after the eruption of Mt. Pinatubo [*McCormick et al.*, 1995]. Often the westerly shear and associated weak ascent lasts for a short period only. E.g., for the trajectories started at 675 K in a westerly shear in July 1987, a few parcels actually descend during the first month; still the median is ascending.

[44] In general, we expect that not only the phase of the QBO influences the distributions, but also the variable phase propagation—a stalled QBO with constant phase over several months will have a different imprint on transport than a rapidly descending QBO that passes over a given level quickly.

[45] Nonetheless, a relation between QBO phase and upward transport was found. In Figure 6, the total ascent over 90 days to the 675-K level is displayed as a function of the QBO phase. The radii of black and colored circles give the annual and seasonal means of the ascent, respectively.

[46] The QBO phase was derived from the zonal wind u and the vertical shear of zonal wind, $u_z = \frac{du}{dz}$ [also see *Huesmann and Hitchman*, 2003]. Consider an idealized QBO that is a harmonic oscillation $u(z, t) = A \sin(kz + \omega t)$. Then $u_z = Ak \cos(kz + \omega t)$ and $\frac{u}{u_z} = k^{-1} \tan(kz + \omega t)$. Hence at a given level $z = 0$, the phase state $\phi = \omega t$ can be obtained from the relation of u and u_z normalized by the ratio of their amplitudes, k^{-1}. The real QBO is unsteady and not harmonic, neither in the vertical nor in time, which is why its phase can hardly be derived from u or u_z alone. However, their standard deviation of σ_u and σ_{uz} offer a robust estimate of their

amplitudes, and thus ϕ can be derived from the combination of u and u_z

$$\tan\phi = \frac{u\sigma_{uz}}{u_z\sigma_u} \tag{1}$$

[47] In other words, in a plane spanned by u (on the ordinate) and u_z (on the abscissa), ϕ is the angle spanned by the abscissa and the point (u_z, u) at any given time. E.g., at the beginning of a westerly phase, u_z is positive but decreasing, and by the time u becomes maximum positive, approaches 0, hence $\phi \to \pi/2$ and (u_z, u) is located on the ordinate. At the time when wind shear becomes easterly, u_z is negative and ϕ enters the second quadrant, and so on.

[48] The phase was computed at the start of the trajectories at the approximated level of release, in this case 675 K. In Figure 6, symbols mark the median and bars show the 10th and 90th percentiles, and colors again distinguish seasons. Clearly, the trajectories of parcels that are released in a westerly shear phase have lower total ascent than the seasonal average, and those released in an easterly shear show above-average ascent. The phase of maximum ascent is shifted toward the easterly phase, as discussed above. While this is true for all four seasons, no significant seasonal dependence of this phase shift is found, more cases would be required to analyze this point.

4. QBO Effect on Horizontal Transport

[49] The analysis of PV gradients at the 600-K level in section 2 suggested a transport barrier at the summer tropical-subtropical edge during the easterly phase of the QBO only. In this section, we elaborate on this finding by studying a methane profile in the CCM simulation with a representation of the QBO and the motion of trajectories based on this run.

[50] In the stratosphere, methane is a well-suited trace gas for transport studies. It has sources only below the tropopause, a long stratospheric lifetime, but also has a sink in the stratosphere. Upon its ascent in the tropical pipe from the tropical tropopause region it is oxidized gradually in the middle and upper stratosphere. Therefore methane concentrations in the extratropics are determined by the descent from above and by isentropic transport from the tropics. Hence there are gradients of the volume mixing ratio in both the horizontal and vertical directions, and variations in vertical and horizontal transport are reflected in methane concentrations. The effects of the QBO on methane are discussed by *Randel et al.* [1998], *Dunkerton* [2001] and *Patra et al.* [2003].

[51] Figure 7a shows the zonally averaged latitudinal profile of the methane volume mixing ratio at 600 K ($\approx$32 hPa) in July for easterly and westerly QBO phases. The blue and orange line are the profiles in the westerly phase of 1990 and the easterly phase of 1989, respectively. The thick cyan line is the July average of the years 1985, 1990, 1995, 1997, and 1999, in which the QBO is in a pronounced westerly phase and the thick red line is the July average of the years 1984, 1989, 1994, 1996, and 1998 with a pronounced easterly QBO phase. The July concentrations averaged from five years are higher than the 1989 and 1990 examples because of the positive methane trend in the stratosphere.
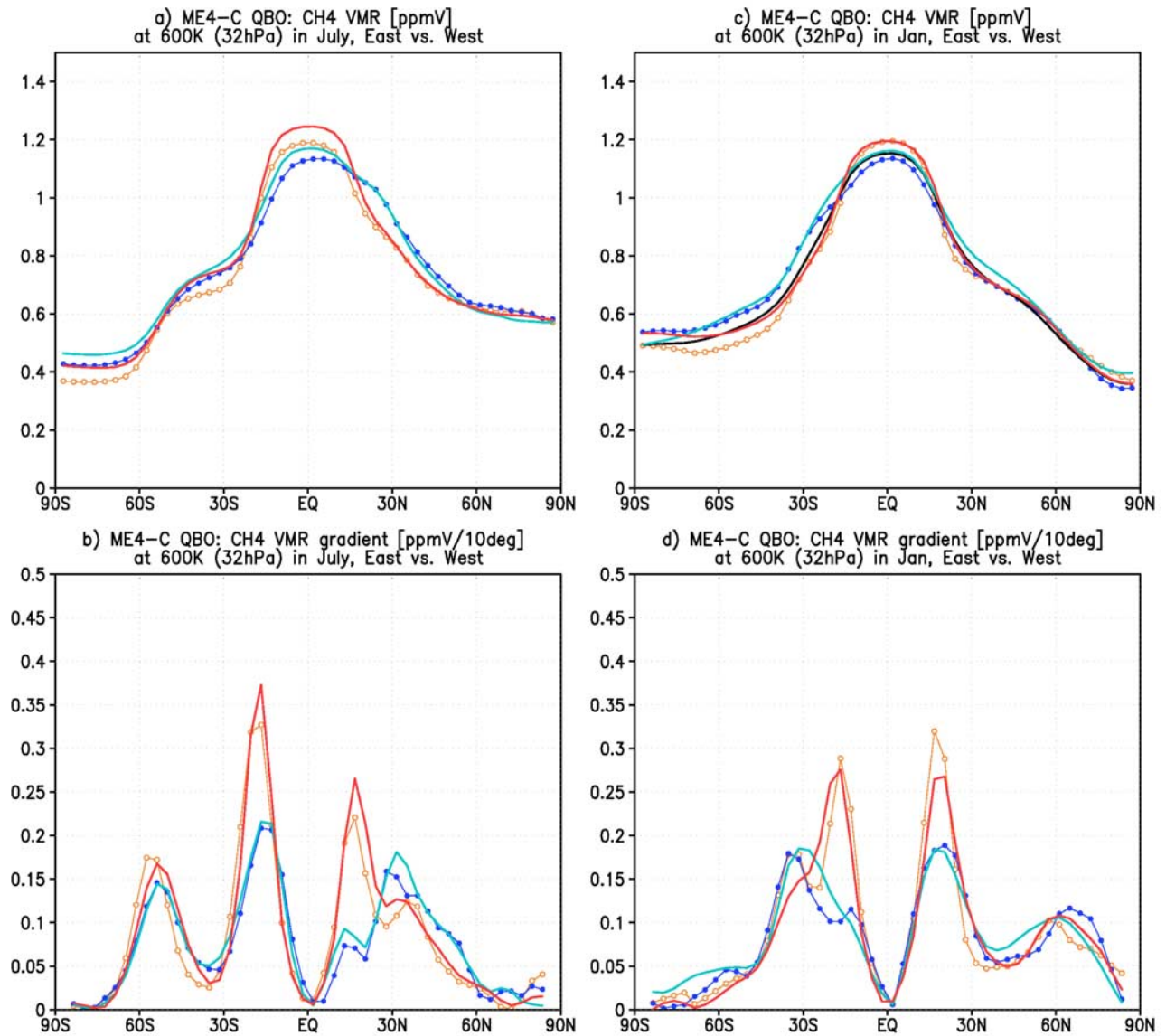
Figure 7. (a) Modeled methane concentration at 600 K (32 hPa) during the westerly phase of the QBO in July 1990 (thin blue line) and during the easterly phase of the QBO in July 1989 (thin orange line). The thick red line gives the average of 5 years when the QBO was easterly in July, the cyan line the average of 5 years with the westerly QBO phase in July. (b) Absolute value of the horizontal gradient of the curves in Figure 7a (ppmv/10°). (c) As in Figure 7a but during the westerly phase of the QBO in January 1988 (thin blue line) and during the easterly phase of the QBO in January 1987 (thin orange line). The thick red line gives the average of 4 years when the QBO was easterly in January, the cyan line the average of 4 years with the westerly QBO phase in January. (b) Absolute value of the horizontal gradient of the curves in Figure 7c (ppmv/10°).

[52] It is evident that in the years with easterly wind the equatorial volume mixing ratio is higher than in the years with westerly wind because of the integral upwelling modulation caused by the SMC, which was described in the previous section, in combination with the vertical gradient of methane. This result is in agreement with the findings of *Randel et al.* [2004].

[53] On the winter hemisphere, the methane profiles look similar in all years. There is a sharp decrease in the subtropics, a rather weak gradient in the midlatitudes between 25°S and 45°S, and a stronger decrease at the Antarctic polar vortex edge. This is in agreement with the conception of a well-mixed surf zone at midlatitudes [*McIntyre and Palmer*, 1984] and transport barriers at the vortex edge [*Nash et al.*, 1996] and in the subtropics [*Gray*, 2000, see also *Plumb*, 2002].

[54] As expected from the PV analysis, there is a considerable difference between easterly and westerly years in the summer hemisphere subtropics, compare the cyan and red lines in Figure 7 between 15 and 40°N. Volume mixing ratios are higher in this region in the westerly cases, especially in the boreal summer case (Figure 7a). This seems to be in
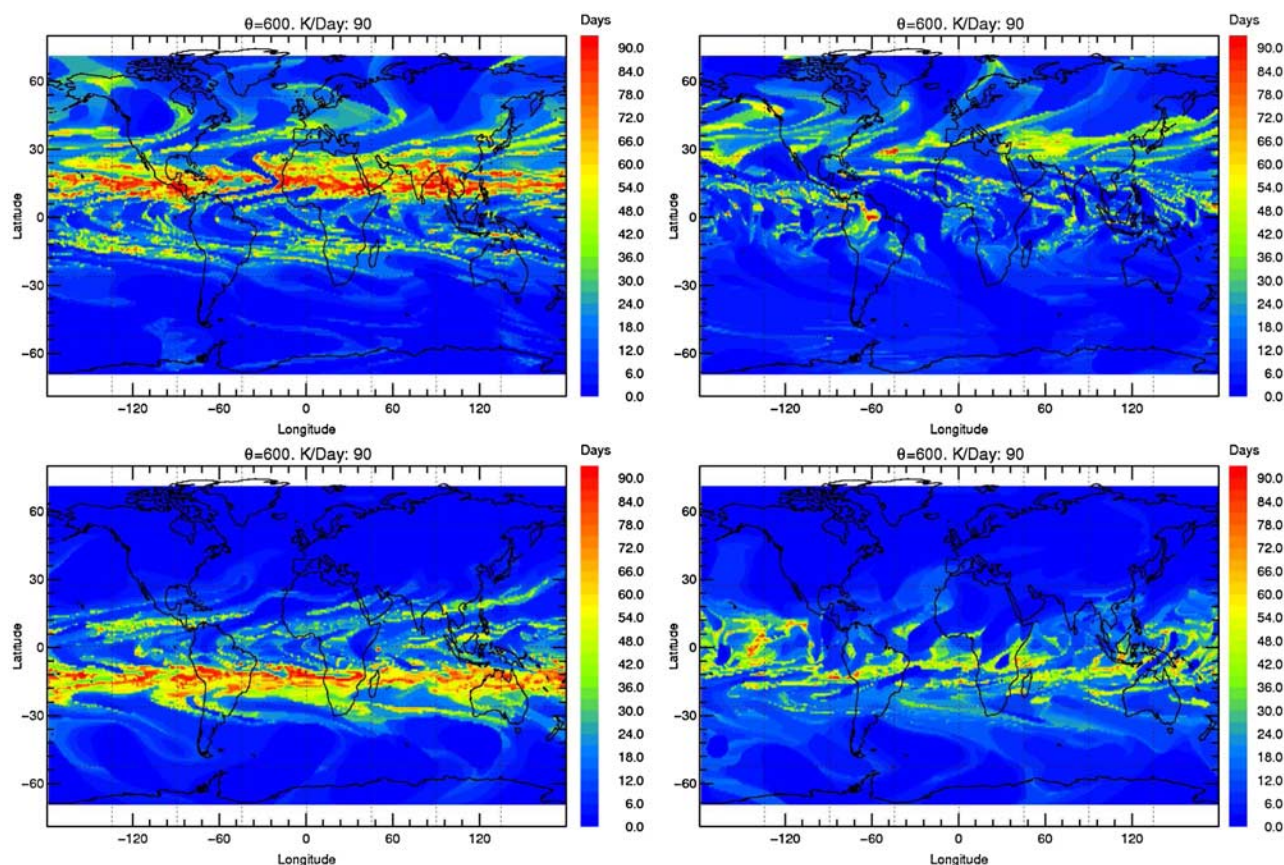
Figure 8. Time out of the last 90 days for which parcels have been in their present latitude range (±5°) before their arrival at 600 K (a) during the easterly phase of the QBO in July 1989, (b) during the westerly phase of the QBO in July 1990, (c) during the easterly phase of the QBO in January 1987, and (d) during the westerly phase of the QBO in January 1988.

contrast to the concept of the SMC, which would predict increased poleward transport during the easterly phase but relative equatorward flow during the westerly phase, thus higher methane in the easterly phase. However, variation of the strength of the transport barrier with QBO phase offers an explanation for this finding. Figures 7b and 7d show the latitudinal gradients of the concentrations given in Figures 7a and 7c. They confirm that there is a significant difference between easterly and westerly years in the summer subtropics at about 15–20°N. The large gradient in easterly years is consistent with the proposed subtropical transport barrier in summer, whereas in westerly years, transport from the tropics into this region appears to be enhanced, causing the higher subtropical methane concentrations with a significantly weaker gradient at 15–20°N.

[55] Figure 7b also shows a 75% higher CH_4 gradient at the winter tropical-subtropical edge in easterly compared to westerly years. It is in part due to the vertical transport effect of the SMC induced by the QBO discussed above, which causes higher tropical concentrations and lower subtropical concentrations in easterly years. This also affects the gradients on the summer hemisphere, but does not explain the strong difference in the northern hemisphere profile found in Figure 7b, where the gradient at the edge in the easterly cases is approximately three times the one in the westerly cases. In the austral summer case (Figure 7d) the picture is similar, the

gradients are higher by 50% on the winter hemisphere but more than doubled on the summer hemisphere. The amounts of these differences depend on the exact phase and strength of the QBO. *O'Sullivan and Chen* [1996] found a similar effect of the QBO on the summer hemisphere for their artificial tracer using an Eulerian transport scheme in a middle atmosphere GCM.

[56] Parcel trajectories can be used in various ways to study transport barriers [e.g., *Bowman*, 1996]. The approach chosen here is to analyze whether the backward trajectories started at a given latitude remain at this latitude during the considered period, that is, whether the air originates from a latitude close to its final latitude or not. If parcels do not move much latitudinally between the start and the end of their trajectories, this indicates a transport barrier, but if they do, it indicates that there is transport in the latitudinal direction.

[57] Figure 8 shows the time air parcels released in boreal and austral summer on the 600 K level at a given horizontal position have remained within a 10° channel around their original latitude during three months of backward trajectory calculations, respectively. In both the easterly (start on 28 July 1989, Figure 8a) and westerly (start on 28 July 1990, Figure 8b) years, air is rapidly removed from its starting latitude in the surf zone on the southern hemisphere and in the Antarctic vortex. If the vortex was circular, our trajectory diagnostic could identify the transport barrier at its edge.
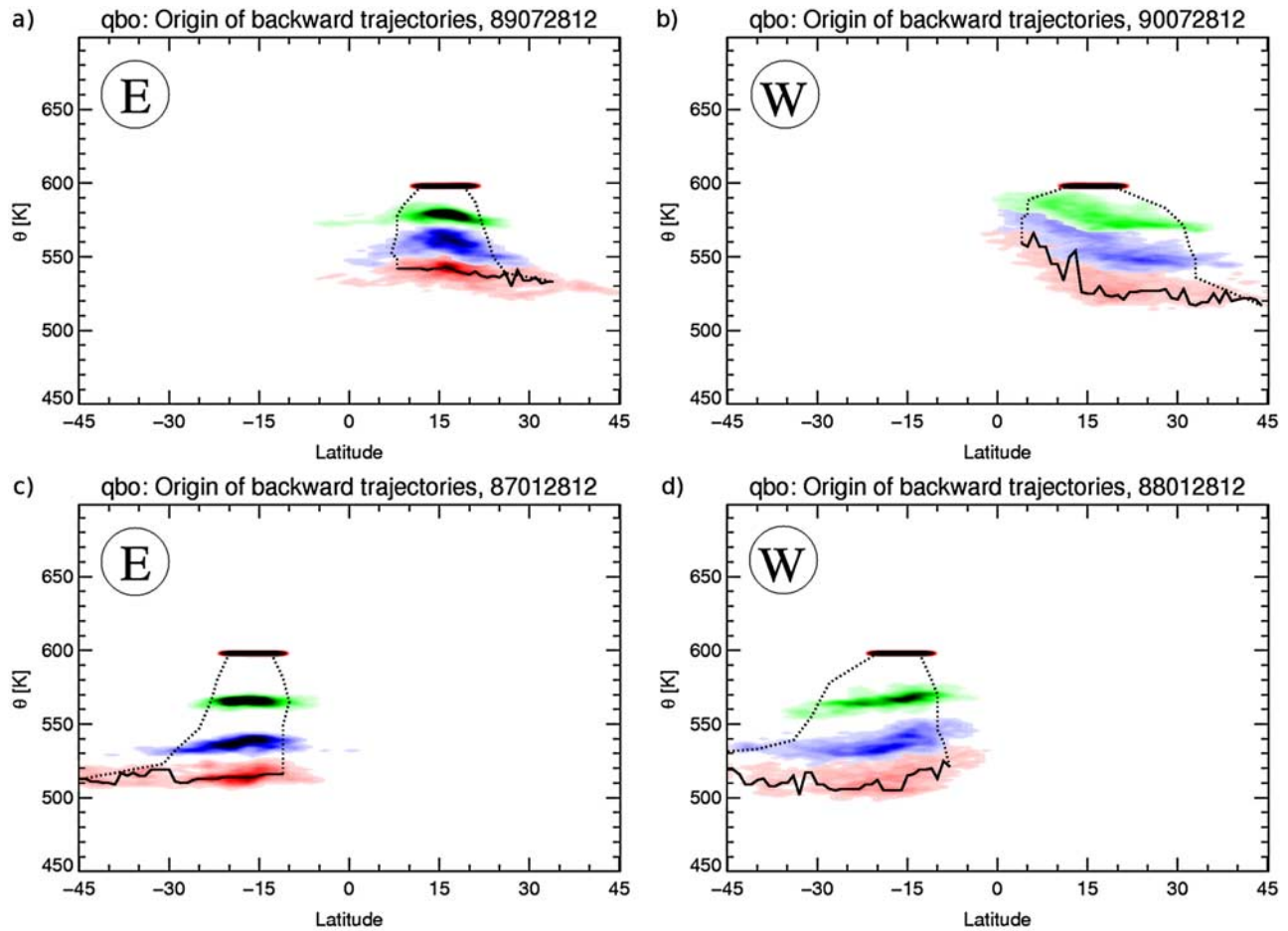
Figure 9. As in Figure 3 but for parcels started at 600 K in the northern subtropics 28 July ((a) easterly wind (1989); (b) westerly wind (1990)) and in the southern subtropics 28 January ((c) easterly wind (1987); (d) westerly wind (1988)). Color scale as in Figure 3.

However, as it is not, each parcel is shifted latitudinally within a few days of its rapid circumpolar motion.

[58] Regarding the misrepresentation of the barrier at the Antarctic vortex, an alternative diagnostic was tested, in which the total time spent in the 10° range of the starting latitude was analyzed. In this case, the vortex is clearly identified, as parcels reenter the starting latitude channel after being deflected by the vortex asymmetry. This diagnostic is however less suitable at lower latitudes, where large-scale mixing, being a counter-indicator of transport barriers, can have the same effect. Moreover, in the tropics the circulation does not show pronounced zonal asymmetries in the altitude range considered, and hence no zonal dependence of the barrier location is expected, in contrast to the vortex.

[59] In the austral summer cases, parcels that start at mid- and high latitudes in the easterly (28 January 1987, Figure 8c) or westerly QBO phase (28 July 1988, Figure 8d), are also rapidly removed from their initial location. On the respective summer hemisphere, the eddy induced mixing is weaker than on the winter hemisphere [Shuckburgh et al., 2001; Allen and Nakamura, 2001] and hence there are occasionally air masses that remain for some time at their original latitude.

[60] In the tropics and—especially summer—subtropics, the effect of the QBO is seen clearly. In the westerly years

(Figures 8b and 8d), although the situations are rather inhomogeneous, some air stays at its original latitude for a month or more during the three months under consideration between 20°S and 30°N, but only within some filaments on a smaller scale than in the summer extratropics.

[61] In the easterly years, however, most of the air parcels retain their location between 10° and 30° on the respective summer hemispheres for the entire period. It is clear that hardly any latitudinal transport takes place under such conditions. Between 20° on the winter hemisphere and 10° on the summer hemisphere though, much fewer air parcels reside around their start location.

[62] An analysis of stream function (given by *Punge and Giorgetta* [2008], Figure A1g) shows that the subtropical air is influenced by the southern winter circulation cell, which, as seen in Figure 4, drags air toward the southern hemisphere. A qualitative explanation of the observed stalling of the parcel trajectories would thus be that the opposed influences of seasonal cycle and QBO cancel, creating a region of little latitudinal motion. The northward flow of the SMC dominates in the tropics but is weaker than the southbound flow by the BDC, which leads to convergence and hence relative subsidence in the barrier region.

[63] In Figure 9, we show an analysis of air parcel transport in the barrier region analogous to the equatorial analysis in
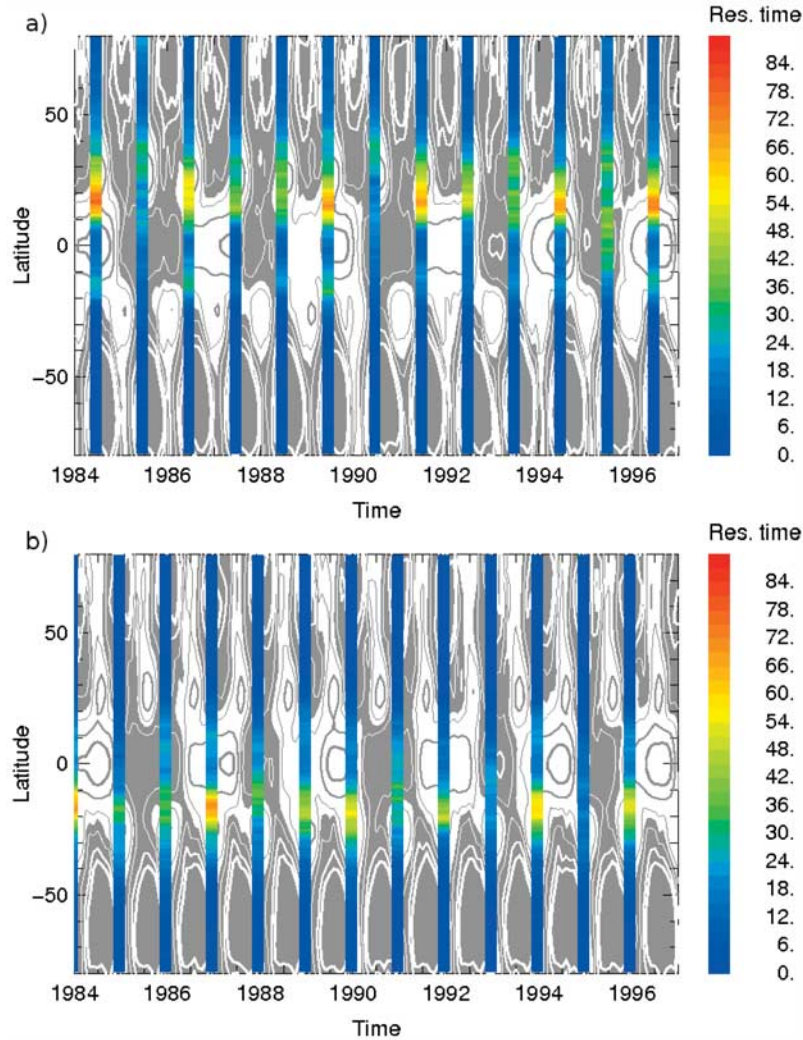
Figure 10. Bars show the zonal mean residence time in a channel of ±5° around the release latitude in days for backward trajectories started on (a) 28 July and (b) 28 January of each year from 1984 to 1996 at the 600-K level. The background shows the zonal mean zonal wind. Easterlies are colored in white with contour levels at −5, −15, and −25 m/s; westerlies in grey with contours at 5, 15, and 25 m/s.

Figures 3 and 4. The distributions of parcels that are started between 12 and 20°N at the 600-K level on 28 July 1989 and 1990 are shown in 30-day intervals in Figures 9a and 9b, respectively. In Figures 9c and 9d, the corresponding austral summer case is given, and distributions of parcels that are released between 12 and 20°S on 28 January 1987 and 1988 are shown. There is little horizontal advection of the parcel cloud during the easterly cases, Figures 9a and 9c, but mean southward advection in the westerly cases, Figures 9b and 9d. Furthermore, in the easterly case, especially for boreal summer, there is evidence for reduced ascent at the barrier location between 15 and 20°N. Compared to the westerly case, total ascent over 90 days of the July trajectories is lower by approximately 15 K or 20%, in support of our reasoning in the last paragraph. This effect is less pronounced in the austral summer cases.

[64] Generally, the absence of net advection does not per se explain the existence of the observed barrier. In Figure 9, we also observed a much higher compactness of the parcel distribution in the easterly QBO cases compared to the westerly QBO cases. We assume that the modulation of the propagation of planetary waves from the winter hemisphere by the presence or absence of an easterly QBO jet is causing this effect. The small-scale eddy transport caused by the dispersion of these waves would hinder the formation of a barrier in the westerly case, even if large-scale transport was negligible.

[65] To provide further evidence for the barrier modulation by the QBO in summer and its presence also on the southern hemisphere, we applied the residence time diagnostic as in Figure 8 to different QBO phases over a longer period and also during austral summer. In Figure 10, the zonal mean of residence times computed as in Figure 8 is displayed in form of a bar that extends over the runtime of the trajectories.

[66] In boreal summer (Figure 10a), situations with reduced horizontal motion at about 15−20°N are found in easterly QBO years as in 1984, 1989, 1994, and 1996, but not in the westerly years 1985, 1990, 1993, and 1995. In situations with no pronounced easterly or westerly QBO phase, such as the westerly and easterly shear phases in 1987 and

1988, residence times are longer in the northern subtropics than elsewhere, but clearly shorter than in the easterly years.

[67] The same picture is found in austral summer (Figure 10b). Regions of high residence time are found at $15-20°S$ for trajectories started in January of 1984, 1987, 1989, 1990, and 1994, when winds are easterly, but are absent in the cases with westerlies as for the trajectories started in January 1986, 1988, 1991, 1993, and 1995. Generally, subtropical residence times are shorter on the southern hemisphere compared to the northern hemisphere, and the QBO-related differences are less pronounced in the southern hemisphere. It appears that the weaker planetary wave forcing on the southern hemisphere compared to the northern one leads to a less pronounced barrier because of the less pronounced wave induced mixing in the surf zone [*Plumb*, 2002].

5. Conclusions

[68] The effect of the QBO on stratospheric transport at low latitudes has been illustrated by means of trajectory calculations based on a general circulation model with representation of the stratospheric circulation and chemistry.

[69] Regarding research question 1 defined above, we find the following.

[70] 1. Ensembles of trajectories running backward over three months following the GCM winds and heating rates show a clear modulation of tropical ascent associated with the QBO independent of the season. Upwelling is enhanced when the vertical wind shear caused by the QBO jets at a selected level is easterly but reduced or even turned to subsidence in westerly shear conditions at the equator as expected because of the secondary meridional circulation of the QBO [*Plumb and Bell*, 1982]. The effect of this circulation anomaly on transport is pronounced in both easterly and westerly shear phases, but as the QBO jets are descending while the air is ascending, the exposition time of individual air parcels to the different shear phases is limited and the differences in integrated ascent over longer periods are smaller than the differences in instantaneous ascent rates. Nonetheless, the effect of the SMC is clearly seen after three months of integration.

[71] 2. Additionally, the phase of maximum integral ascent over the last three months lags the phase of maximum easterly shear and thus the associated maximum instantaneous ascent by several months; the exact amount of this lag however varies with the rate of downward propagation of the QBO. In fact, the impact of the changing QBO phase is stronger in the cases with easterly wind shear or easterly wind, which have a higher total ascent than the westerly wind shear or westerly wind cases. Hence the phase relationship between the QBO phase as diagnosed from wind and wind shear to the ascent variation over 90 days will generally not be linear but will vary with the QBO cycle. This should be taken into account in studies that diagnose the effect of the QBO on the distributions of long-lived trace gases as methane [*Randel et al.*, 1998] or N_2O [*Schoeberl et al.*, 2008], or, potentially, SF_6 [*Stiller et al.*, 2008].

[72] 3. The trajectory calculations also show that the effect of the SMC on upwelling is strongest in a narrow region around the equator, but isentropic exchange leads to a homogenization of the ascent in the equatorial region on a

time scale of a few months. During solstitial seasons, the asymmetry of the BDC leads to general flow toward the winter hemisphere and a larger fraction of the air stems from the summer hemisphere with rather high total ascent. The QBO modulation of equatorial ascent appears to be largely unaffected by season. Especially in the westerly shear phase this leads to a large spread in the ascent histories of tropical air parcels.

[73] 4. The advection by the horizontal part of the SMC is less easily identified from the trajectory distributions, probably because isentropic transport is less uniform than the vertical transport. As suggested by *Ribera et al.* [2004], the horizontal circulation anomaly due to the SMC may not always coincide with the phases of the strongest easterly and westerly jets (see Figure 1) that were selected here. Nonetheless, especially in the equinoctial seasons, the width of the latitude range, from which most parcels originate, varies clearly with the phase of the QBO and is narrowest in the selected Easterly phase, as expected.

[74] Regarding our research question 2, we conclude the following.

[75] 1. In the solstitial seasons, the circulation anomaly toward the winter pole due to the hemispheric asymmetry of the BDC is superimposed to the symmetric horizontal branch of the SMC. This leads to zones with no large-scale latitudinal transport in the near subtropics at around $15-20°$ latitude on the summer hemisphere during the easterly phase. As evident from Figure 8, the trajectories of parcels in this region show almost no latitudinal transport in this situation at all. Following the same reasoning as above, one would expect a similar zone of no large-scale latitudinal transport in the winter subtropics during the westerly phase, which is however not evident in Figure 8. It seems likely that the poleward flow of the BDC dominates over the equatorward flow because of the SMC in this situation.

[76] 2. Furthermore, in the absence of an easterly tropical jet, planetary wave-induced isentropic mixing leads to dispersion of air parcels at these latitudes even if net advection is zero. This is supported by the high mixing anomaly in the westerly phase found by *Garny et al.* [2007]. In the easterly phase on the summer hemisphere, however, a transport barrier develops and this kind of dispersion is absent. As suggested by earlier studies in an Eulerian framework [*Haynes and Shuckburgh*, 2000; *Shuckburgh et al.*, 2001], the fact that planetary waves cannot enter the easterly QBO jets appears to be the reason for the evolution of that barrier.

[77] 3. The barrier separates the extratropics, where extratropical waves drive isentropic transport in the surf zone [*McIntyre and Palmer*, 1984], from the tropical domain with easterly winds and little influence of extratropical waves. While one would expect this barrier to be stronger in winter when the wave forcing and surf zone mixing is stronger, our results suggest that the poleward general circulation hinders the evolution of a stationary subtropical barrier in these cases. In the westerly QBO phase, the separation of the tropical and extratropical domains is weaker and the mean latitudinal flow does not allow for the evolution of a barrier. To support this reasoning on the tropical-subtropical transport barrier, further, more detailed studies would be desirable. In particular, the respective roles of isentropic mixing and horizontal advection deserve further investigation. More advanced statistical evaluation techniques of parcel motion may be valuable

tools here. A quantification of the barrier strength from its effects on trace gas distributions observed in the atmosphere is needed to validate the model results presented in this work. Also, its vertical extent needs to be analyzed, which was not done in this study, where trajectories are released only at a few levels.

[78] Trajectory calculations based on a general circulation model proved to be an effective tool for transport diagnostics. One needs to be aware that the CCM used here has its specific shortcomings, as mentioned in section 2.1, and hence the findings of this study may differ from reality in details, such as the exact location of the barrier or hemispheric asymmetries. Nonetheless, the consistent dynamical fields of the CCM, as opposed to reanalyses or operational analyses in which many different observations are assimilated, are suitable for accurate quantification of the QBO's effect on transport in the stratosphere by means of Lagrangian analysis. When the present setup is extended by including the mixing and chemistry modules of the CLaMS model, this allows to study effects of the QBO on small-scale mixing, age of air and trace gas distributions from a Lagrangian point of view.

References

Allen, D. R., and N. Nakamura (2001), A seasonal climatology of effective diffusivity in the stratosphere, *J. Geophys. Res.*, *106*(D8), 7917–7936.

Angell, J. K., and J. Korshover (1964), Quasi-biennial variations in temperature, total ozone, and tropopause height, *J. Atmos. Sci.*, *21*, 479–492.

Baldwin, M. P., et al. (2001), The quasi-biennial oscillation, *Rev. Geophys.*, *39*(2), 179–229.

Bowman, K. P. (1996), Rossby wave phase speeds and mixing barriers in the stratosphere. part I: Observations, *J. Atmos. Sci.*, *53*, 905–916.

Chen, P. (1996), The influences of zonal flow on wave breaking and tropical-extratropical interaction in the lower stratosphere, *J. Atmos. Sci.*, *53*(16), 2379–2392.

Dunkerton, T. J. (2001), Quasi-biennial and subbiennial variations of stratospheric trace constituents derived from HALOE observations, *J. Atmos. Sci.*, *58*(1), 7–25.

Eyring, V., et al. (2006), Assessment of temperature, trace species and ozone in chemistry-climate model simulations of the recent past, *J. Geophys. Res.*, *111*, D22308, doi:10.1029/2006JD007327.

Garny, H., G. E. Bodecker, and M. Dameris (2007), Trends and variability in stratospheric mixing: 1979–2005, *Atmos. Chem. Phys.*, *7*, 5611–5624.

Giorgetta, M. A., and L. Bengtsson (1999), Potential role of the quasi-biennial oscillation in stratosphere-troposphere exchange as found in water vapor in general circulation model experiments, *J. Geophys. Res.*, *104*(D6), 6003–6020.

Gray, L. J. (2000), A model study of the influence of the quasi-biennial oscillation on trace gas distributions in the middle and upper stratosphere, *J. Geophys. Res.*, *105*(D4), 4539–4552, doi:10.1029/1999JD900320.

Haynes, P., and E. Shuckburgh (2000), Effective diffusivity as a diagnostic of atmospheric transport: 1. Stratosphere, *J. Geophys. Res.*, *105*(D18), 22,777–22,794.

Haynes, P. H., M. E. McIntyre, T. G. Shepherd, C. J. Marks, and K. P. Shine (1991), On the "downward control" of extratropical diabatic circulations by Eddy-induced mean zonal forces, *J. Atmos. Sci.*, *48*, 651–680.

Hines, C. O. (1997a), Doppler spread parameterization of gravity wave momentum deposition in the middle atmosphere. part I: Basic formulation, *J. Atmos. Sol. Terr. Phys.*, *59*, 371–386.

Hines, C. O. (1997b), Doppler spread parameterization of gravity wave momentum deposition in the middle atmosphere. part II: Broad and quasi monochromatic spectra and implementation, *J. Atmos. Sol. Terr. Phys.*, *59*, 387–400.

Huesmann, A. S., and M. H. Hitchman (2003), The 1978 shift in the NCEP reanalysis stratospheric quasi-biennial oscillation, *Geophys. Res. Lett.*, *30*(2), 1048, doi:10.1029/2002GL016323.

Jackman, C. H., E. L. Fleming, S. Chandra, D. B. Considine, and J. E. Rosenfield (1996), Past, present, and future modeled ozone trends with comparisons to observed trends, *J. Geophys. Res.*, *101*(D22), 28,753–28,768.

Khosrawi, F., J.-U. Grooß, R. Müller, P. Konopka, W. Kouker, R. Ruhnke, T. Reddmann, and M. Riese (2005), Intercomparison between Lagrangian and Eulerian simulations of the development of mid-latitude streamers as observed by CRISTA, *Atmos. Chem. Phys.*, *5*, 85–95.

Kirchner, I., G. L. Stenchikov, H.-F. Graf, A. Robock, and J. C. Antuña (1999), Climate model simulation of winter warming and summer cooling following the 1991 Mount Pinatubo volcanic eruption, *J. Geophys. Res.*, *104*(D16), 19,039–19,055.

Konopka, P., et al. (2007), Contribution of mixing to upward transport across the tropical tropopause layer (TTL), *Atmos. Chem. Phys.*, *7*, 3285–3308.

Lean, J. L., G. J. Rottman, H. L. Kyle, T. N. Woods, J. R. Hickey, and L. C. Puga (1997), Detection and parameterization of variations in solar mid- and near-ultraviolet radiation (200–400 nm), *J. Geophys. Res.*, *102*(D25), 29,939–29,956.

Manzini, E., and N. A. McFarlane (1998), The effect of varying the source spectrum of a gravity wave parameterization in a middle atmosphere general circulation model, *J. Geophys. Res.*, *103*(D24), 31,523–31,539.

Manzini, E., N. A. McFarlane, and C. McLandress (1997), Impact of the Doppler spread parameterization on the simulation of the middle atmosphere circulation using the MA/ECHAM4 general circulation model, *J. Geophys. Res.*, *102*(D22), 25,751–25,762.

Manzini, E., B. Steil, C. Brühl, M. A. Giorgetta, and K. Krueger (2003), A new interactive chemistry-climate model: Sensitivity of the middle atmosphere to ozone depletion and increase in greenhouse gases and implications for recent stratospheric cooling, *J. Geophys. Res.*, *108*(D14), 4429, doi:10.1029/2002JD002977.

McCormick, M. P., L. W. Thomason, and C. R. Trepte (1995), Atmospheric effects of the Mt Pinatubo eruption, *Nature*, *373*, 399–404, doi:10.1038/373399a0.

McFarlane, N. A. (1987), The effect of orographically exited gravity drag on the general circulation of the lower stratosphere and troposphere, *J. Atmos. Sci.*, *44*, 1775–1800.

McIntyre, M. E., and T. N. Palmer (1984), The "surf zone" in the stratosphere, *J. Atmos. Terr. Phys.*, *46*, 825–849.

McKenna, D. S., P. Konopka, J.-U. Grooß, G. Günther, R. Müller, R. Spang, D. Offermann, and Y. Orsolini (2002), A new chemical Lagrangian model of the stratosphere (CLaMS): 1. Formulation of advection and mixing, *J. Geophys. Res.*, *107*(D16), 4309, doi:10.1029/2000JD000114.

Mote, P. W., K. H. Rosenlof, M. E. McIntyre, E. S. Carr, J. C. Gille, J. R. Holton, J. S. Kinnersley, H. C. Pumphrey, J. M. Russell III, and J. W. Waters (1996), An atmospheric tape recorder: The imprint of tropical tropopause temperatures on stratospheric water vapor, *J. Geophys. Res.*, *101*(D2), 3989–4006.

Nash, E. R., P. A. Newman, J. E. Rosenfield, and M. R. Schoeberl (1996), An objective determination of the polar vortex using Ertel's potential vorticity, *J. Geophys. Res.*, *101*(D5), 9471–9478.

Neu, J. L., L. C. Sparling, and R. A. Plumb (2003), Variability of the subtropical edges in the stratosphere, *J. Geophys. Res.*, *108*(D15), 4482, doi:10.1029/2002JD002706.

Niwano, M., K. Yamazaki, and M. Shiotani (2003), Seasonal and QBO variations of ascent rate in the tropical lower stratosphere as inferred from UARS HALOE trace gas data, *J. Geophys. Res.*, *108*(D24), 4794, doi:10.1029/2003JD003871.

O'Sullivan, D., and P. Chen (1996), Modelling the quasi-biennial oscillation's influence on isentropic transport in the subtropics, *J. Geophys. Res.*, *101*(D3), 6811–6821.

Patra, P. K., S. Lal, S. Venkataramani, and D. Chand (2003), Halogen Occultation Experiment (HALOE) and balloon-borne in situ measurements of methane in stratosphere and their relation to the quasi-biennial oscillation (QBO), *Atmos. Chem. Phys.*, *3*(4), 1051–1062.

Plumb, R. A. (2002), Stratospheric transport, *J. Meteorol. Soc. Jpn.*, *80*(4B), 793–809.

Plumb, R. A., and R. C. Bell (1982), A model of the quasi-biennial oscillation on an equatorial beta-plane, *Q. J. R. Meteorol. Soc.*, *108*(456), 335–352.

Polvani, L. M., D. W. Waugh, and R. A. Plumb (1995), On the subtropical edge of the stratospheric surf zone, *J. Atmos. Sci.*, *52*, 1288–1309.

Punge, H. J., and M. A. Giorgetta (2008), Net effect of the QBO in a chemistry-climate model, *Atmos. Chem. Phys. Disc.*, *8*, 12,115–12,162.

Randel, W. J., F. Wu, J. W. Russel, A. Roche, and J. Waters (1998), Seasonal cycles and QBO variations in stratospheric CH₄ and H₂O observed in UARS HALOE data, *J. Atmos. Sci.*, *55*, 163–185.

Randel, W. J., F. Wu, S. J. Oltmans, K. Rosenlof, and G. E. Nedoluha (2004), Interannual changes of stratospheric water vapor and correlations with tropical tropopause temperatures, *J. Atmos. Sci.*, *61*, 2133–2147.

Rayner, N. A., D. E. Parker, E. B. Horton, C. K. Folland, L. V. Alexander, D. P. Rowell, E. C. Kent, and A. Kaplan (2003), Global analyses of sea surface temperature, sea ice, and night marine air temperature since the late nineteenth century, *J. Geophys. Res.*, *108*(D14), 4407, doi:10.1029/2002JD002670.

Reed, R. J. (1964), A tentative model of the 26-month oscillation in tropical latitudes, *Q. J. R. Meteorol. Soc.*, *90*, 441–466, doi:10.1002/qj.49709038607.

Ribera, P., C. Peña-Ortiz, R. Garcia-Herrera, D. Gallego, L. Gimeno, and E. Hernández (2004), Detection of the secondary meridional circulation associated with the quasi-biennial oscillation, *J. Geophys. Res.*, *109*(D18), D18112, doi:10.1029/2003JD004363.

Roeckner, E., L. Bengtsson, J. Feichter, J. Lelieveld, and H. Rodhe (1999), Transient climate change simulations with a coupled atmosphere-ocean GCM including the tropospheric sulfur cycle, *J. Clim.*, *12*, 3004–3032.

Roeckner, E., et al. (1996), The atmospheric general circulation model ECHAM4: Model description and simulation of present-day climate, *Max-Planck-Institut für Meteorologie, Rep. 218*, 90 pp., Hamburg, Germany.

Schoeberl, M. R., et al. (2008), Qbo and annual cycle variations in tropical lower stratosphere trace gases from haloe and aura MLS observations, *J. Geophys. Res.*, *113*, D05301, doi:10.1029/2007JD008678.

Shuckburgh, E., W. Norton, A. Iwi, and P. Haynes (2001), Influence of the quasi-biennial oscillation on isentropic transport and mixing in the tropics and subtropics, *J. Geophys. Res.*, *106*(D13), 14,327–14,338.

Steil, B., M. Dameris, C. Brühl, P. J. Crutzen, V. Grewe, M. Ponater, and R. Sausen (1998), Development of a chemistry module for GCMs: First results of a multiannual integration, *Ann. Geophys.*, *16*(2), 205–228.

Steil, B., C. Brühl, E. Manzini, P. J. Crutzen, J. Lelieveld, P. J. Rasch, E. Roeckner, and K. Krueger (2003), A new interactive chemistry-climate model: 1. Present-day climatology and interannual variability of the mid-
dle atmosphere using the model and 9 years of HALOE/UARS data, *J. Geophys. Res.*, *108*(D9), 4290, doi:10.1029/2002JD002971.

Steinbrecht, W., et al. (2006), Interannual variation patterns of total ozone and lower stratospheric temperature in observations and model simulations, *Atmos. Chem. Phys.*, *6*, 349–374.

Stiller, G. P., et al. (2008), Global distribution of mean age of stratospheric air from MIPAS SF6 measurements, *Atmos. Chem. Phys.*, *8*(3), 677–695.

Tian, W., M. P. Chipperfield, L. J. Gray, and J. M. Zawodny (2006), Quasi-biennial oscillation and tracer distributions in a coupled chemistry-climate model, *J. Geophys. Res.*, *111*, D20301, doi:10.1029/2006JD006871.

Tourpali, K., C. J. E. Schuurmans, R. van Dorland, B. Steil, and C. Brühl (2003), Stratospheric and tropospheric response to enhanced solar UV radiation: A model study, *Geophys. Res. Lett.*, *30*(5), 1231, doi:10.1029/2002GL016650.

Trepte, C. R., and M. H. Hitchman (1992), Tropical stratospheric circulation deduced from satellite aerosol data, *Nature*, *355*, 626–628, doi:10.1038/355626a0.

Waugh, D. W. (1996), Seasonal variation of isentropic transport out of the tropical stratosphere, *J. Geophys. Res.*, *101*(D2), 4007–4024.

World Meteorological Organization (WMO) (2003), Scientific assessment of ozone depletion: 2002, *Global Ozone Research and Monitoring Project, Rep. 47*, 498 pp., Geneva, Switzerland.

_____

M. A. Giorgetta and H. J. Punge, Atmosphere in the Earth System, Max Planck Institute for Meteorology, Bundesstr. 53, Hamburg D-20146, Germany. (heinzjuergen.punge@zmaw.de)

P. Konopka and R. Müller, Institut für Chemie und Dynamik der Geosphäre, ICG-1: Stratosphäre, Forschungszentrum Jülich GmbH, D-52428 Jülich, Germany.